Magnetic behavior of Fe(Se,Te) systems: First-principles calculations

Hongliang Shi,[1] Zhong-Bing Huang,[2,a)] John S. Tse,[3] and Hai-Qing Lin[1,b)]
[1]*Beijing Computational Science Research Center, Beijing 100084, People's Republic of China*
[2]*Faculty of Physics and Electronic Technology, Hubei University, Wuhan 430062, People's Republic of China*
[3]*Department of Physics and Engineering Physics, University of Saskatchewan, Saskatoon, Saskatchewan S7N 5E2, Canada*

(Received 17 March 2011; accepted 13 July 2011; published online 24 August 2011)

The magnetic behaviors in Fe(Se,Te) systems have been investigated systematically using density functional calculations. At the experimental lattice parameters, the ground state is found to be in the double stripe magnetic phase for FeTe but in the single stripe magnetic phase for FeSe and $FeSe_{0.5}Te_{0.5}$, and there is no preference in the different easy axes of magnetization. Substitution of Se by Te enlarges the size of the Fermi surface in $FeSe_{0.5}Te_{0.5}$, resulting in a stronger nesting effect and thus enhancing the superconductivity. It is found that the double stripe order in $FeTe_{1-x}Se_x$ changes to the single stripe order when $x > 0.18$. Spiral calculations on $FeSe_{0.5}Te_{0.5}$ show that the lowest energy is at the commensurate point $\vec{Q} = (0.5,0.5)$, accompanied by additional local minima at two incommensurate points near $\vec{Q} = (0.5,0.5)$. This observation is consistent with the experimentally observed positions of low energy magnetic excitations. Geometry optimization calculations show that the tetragonal cell relaxes to orthorhombic and monoclinic cells for FeSe and FeTe, respectively, but remains unchanged for $FeSe_{0.5}Te_{0.5}$. © *2011 American Institute of Physics*. [doi:10.1063/1.3624759]

I. INTRODUCTION

The discovery of the LaFeAs(O,F) superconductor with $T_c = 26$ K,[1] representing a new superconducting family, is a great surprise to scientists. Not long after this discovery was made, another superconductor, α-FeSe with $T_c \sim 8$ K, that consisted of the same square planar sheets of tetrahedrally coordinated Fe was reported.[2] Superconductivity is not found in the parent FeTe, but upon replacing Te with Se, the long-ranged antiferromagnetic (AFM) order is suppressed and superconductivity is observed.[3] Subsequent theoretical investigations showed that both LaFeAsO (Ref. 4) and FeSe (Ref. 5) are not conventional superconductors that can be described in terms of standard electron-phonon theory. As of now, the property of the superconducting state and pairing mechanism are still under debate. A widely accepted idea is that iron-based high T_c superconductivity has a close association with the magnetism characterized by the same Fe square planar sheets.

For the ground state of the parent compounds of FeAs-based pnictides, the single stripe collinear AFM order with a (0.5,0.5) vector was observed,[6–9] whereas FeTe is in the double stripe collinear AFM state with a (0.5,0) vector.[3,10,11] Considering that density functional studies[5] showed that the Fermi surface of the iron chalcogenides Fe(S, Se, Te) is similar to that of iron pnictides, the magnetic order or spin-density wave (SDW) instability induced by Fermi surface nesting should be the same in these two systems. However, as mentioned above for FeTe, its magnetic order vector (0.5,0) does not match the nested vector (0.5,0.5), which has be explained by exchange parameters between Fe-Fe neighbors.[11] In $FeTe_{1-x}Se_x$, there exist competing (0.5,0.5) and (0.5,0) magnetic ordering vectors, and the former becomes more stable than the latter with increasing Se content, as suggested in previous studies.[3,12]

Apart from the characterization of the magnetic ground state, a deep understanding of the magnetic excitation spectrum is essential in order to achieve a comprehensive understanding of the relationship between magnetism and superconductivity in iron-based superconductors. Many works have been performed to study the magnetic resonance feature in $Fe_{1+y}Te_{1-x}Se_x$.[13–16] In contrast to the magnetic ordering vector $\vec{Q} = (0.5,0)$ of the parent compound $FeTe_{1+y}$,[10] a quasi-two-dimensional spin resonance was found near $\vec{Q} = (0.5,0.5)$ in the superconducting sample $FeTe_{0.6}Se_{0.4}$.[13] This resonant magnetic excitation was also observed in $BaFe_{1.84}Co_{0.16}As_2$,[17] indicating that Fe-based superconductors might share a common origin of superconductivity.[18] In $FeSe_{0.5}Te_{0.5}$, besides the commensurate resonance at $\vec{Q} = (0.5,0.5)$, two incommensurate excitations were also observed at 0.409 and 0.638 reciprocal lattice units.[14] It has been argued that spin excitations near $\vec{Q} = (0.5,0.5)$ are important for pairing,[17] and if the incommensurate excitations are close to $\vec{Q} = (0.5,0.5)$, better superconducting properties would be realized.[14] Theses results demonstrate that the behavior of resonance and incommensurate magnetism is rather unusual and deserving of further studies.[14]

In order to gain insight into the relation between the magnetic and superconducting properties of Fe(Se,Te) systems, a systematic investigation of the magnetic anisotropy energy, magnetic order, Fermi surface, and spiral spin structures in these systems was performed. It is shown that the ferromagnetic (FM) state in FeSe relaxed to a nonferromagnetic state, but this did not occur in FeTe. Moreover, the ground state for FeTe is double stripe magnetic, but the single stripe

a)Author to whom correspondence should be addressed. Electronic mail: huangzb@hubu.edu.cn.
b)Electronic mail: haiqing0@csrc.ac.cn.

 © 2011 American Institute of Physics

Downloaded 24 Aug 2011 to 166.111.32.163. Redistribution subject to AIP license or copyright; see http://jap.aip.org/about/rights_and_permissions

magnetic phase is found for FeSe and $FeSe_{0.5}Te_{0.5}$. Perhaps most interesting, spiral calculations on $FeSe_{0.5}Te_{0.5}$ successfully predicted the lowest energy state at the commensurate point $\vec{Q} = (0.5,0.5)$, where the resonance is observed in the spin excitation spectrum. Consistent with neutron scattering experiments, two low energy incommensurate excitations near $\vec{Q} = (0.5,0.5)$ were found in the spin spiral states. Furthermore, our study of the magnetic order evolution in $FeTe_{1-x}Se_x$ as a function of x shows that as x exceeds a critical value of 0.18, the single stripe magnetic phase becomes more stable than that of the double stripe. The paper is organized as follows: In Sec. II, the computational method is briefly described. In Sec. III, the results obtained are described and discussed. In Sec. IV, the conclusions are presented.

II. DETAILS OF CALCULATION

Our first principles calculations are performed using the density functional theory in the generalized gradient approximation (GGA) of the Perdew–Burke–Ernzerhof functional[19] for the exchange correlation potential and the projector augmented wave[20] method as implemented in the Vienna Ab Initio Simulation package.[21] The electron wave function was expanded in a plane wave basis set with an energy cutoff of 500 eV. The structures of the system studied were fully relaxed until the quantum mechanical forces acting on the atoms were less than 0.001 eV/Å. For the tetragonal unit cell in spin spiral calculation, a $14 \times 14 \times 10$ Monkhorst-Pack k-point mesh was used. For the $2 \times 2 \times 1$ magnetic cell, a $4 \times 4 \times 7$ Monkhorst-Pack k-point mesh was used. Convergence in the total energies was checked carefully. For the density of states (DOS) calculation, a $7 \times 7 \times 9$ k-point mesh was used.

III. RESULTS AND DISCUSSIONS

To determine the magnetic states of FeSe, FeTe, and $FeTe_{1-x}Se_x$, following previous work,[12] a commensurate $2 \times 2 \times 1$ magnetic cell for the single-stripe (AFM1) and double-stripe (AFM2) spin configurations as shown in Figs. 1(a) and 1(b) was used. Experimental lattice parameters were employed in the calculations,[5,11,12,22] but the atomic positions were optimized. For comparison, the FM state and the non-spin polarized (NSP) state for FeSe and FeTe were also examined. Because the magnetic moment often prefers one specific direction, i.e., the easy axis, and not an isotropic arrangement, the total energies of the magnetic states in different axes of magnetization were calculated. Higher-order corrections from spin-orbit coupling were not included as suggested in Ref. 23.

A. Magnetic properties and electronic structure of FeSe and FeTe

The calculated total energies and magnetic moments/Fe (μ_B) in the NSP, FM, AFM1, and AFM2 magnetic configurations for FeSe and FeTe are collected in Table I. Here, the energies are referenced with respect to the ground state of each system. In FM calculations, an initial magnetic moment was assumed. However, after relaxation without a constraint on the magnetic moment, the FM phase relaxed to the NSP state for FeSe. In contrast, the converged magnetic state of FeTe is still ferromagnetically coupled with a moment of 1.12 μ_B/Fe and an energy that is 0.12 eV higher than that of the NSP state. The results are consistent with previous observations showing that FM instability does not exist in FeSe, whereas a borderline FM tendency exists in FeTe,[5] which can be attributed to a higher value of the density of states $N(E_F)$ at the Fermi energy in FeTe, as discussed below.

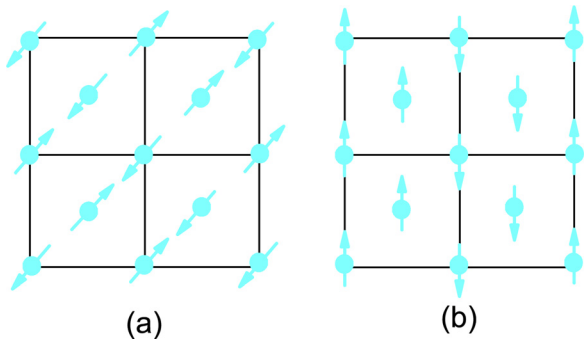

FIG. 1. (Color online) Schematic in-plane AFM spin arrangements in (a) a single stripe structure for FeSe (AFM1) and (b) a double stripe structure for FeTe (AFM2).

For FeSe, the ground state is AFM1 with a magnetic moment of 2.01 μ_B/Fe. This is consistent with the calculated results reported in Ref. 11. The magnetic anisotropy energy in the AFM1 of FeSe does not show any dependence on or preference for the easy axes along the a, b, c, and [110] directions. In AFM2, the calculations reveal a weak dependence on the easy axis, with the relative energy varying from 640 to 658 meV and the magnetic moment from 0.004 to 0.56 μ_B. The ground state of FeTe is in the double-stripe like AFM2 phase and, similar to FeSe, the total energy has no preference for the easy axes. The corresponding magnetic moment is 2.36 μ_B. The AFM1 phase of FeTe has a higher energy of 124 meV and a moment of 2.16 μ_B/Fe in the same directions except for c, along which the energy is 659 meV higher than in AFM2 and the moment is 1.92 μ_B/Fe.

The local spin density approximation (LSDA) was also tested. The common trend of the GGA often overestimating the magnetic moments relative to the LDSA in FeAs superconductors[23,24] is reproduced. For FeSe, the LSDA results show that the total energies of the AFM1 and AFM2 configurations are almost degenerated. In FeTe, the LSDA obtained ground state is an AFM1 configuration, in contrast to the experimental results.[3,10] Therefore, only the GGA results are presented in this work.

In order to gain insight into the magnetic behaviors in FeSe and FeTe, the DOS and orbital-resolved Fe d and chalcogenides p partial density of states (PDOS) in AFM1 and AFM2 are shown in Fig. 2. A comparison of the DOS in Figs. 2(a) and 2(b) for FeSe in AFM1 and AFM2 indicates that the total DOS at the Fermi level is relatively low in the AFM1 ground state. This phenomenon was also observed in $La(O_{1-x}F_x)FeAs$.[9] The main feature of the total DOS in AFM2 with a small magnetic moment is similar to that observed in the nonmagnetic state.[5] In addition, the

Downloaded 24 Aug 2011 to 166.111.32.163. Redistribution subject to AIP license or copyright; see http://jap.aip.org/about/rights_and_permissions

TABLE I. Calculated total energies for FeSe, FeTe, and $FeSe_{0.5}Te_{0.5}$ in the FM, AFM1, and AFM2 magnetic configurations ($2 \times 2 \times 1$ magnetic cell) as well as in the NSP state. In the AFM1 and AFM2 magnetic states, the results with easy axes along the *a*, *b*, *c*, and [110] directions are shown. "Isotropic" in the third column ("Axis") stands for an isotropic arrangement of magnetic moments in the corresponding magnetic configuration.

System	Arrangement	Axis	ΔE (meV)	M (μ_B)
FeSe	FM	Isotropic	637	0.00
	NSP		637	
	AFM1	Isotropic	0.0	2.01
	AFM1	*a*	0.0	2.01
	AFM1	*b*	0.0	2.01
	AFM1	*c*	0.0	2.01
	AFM1	[110]	0.0	2.01
	AFM2	Isotropic	641	0.26
	AFM2	*a*	658	0.56
	AFM2	*b*	640	0.004
	AFM2	*c*	642	0.34
	AFM2	[110]	644	0.35
FeTe	FM	Isotropic	1528	1.12
	NSP		1408	
	AFM1	Isotropic	124	2.16
	AFM1	*a*	124	2.16
	AFM1	*b*	124	2.16
	AFM1	*c*	659	1.92
	AFM1	[110]	124	2.16
	AFM2	Isotropic	0.0	2.36
	AFM2	*a*	0.0	2.36
	AFM2	*b*	0.0	2.36
	AFM2	*c*	0.0	2.36
	AFM2	[110]	0.0	2.36
$FeSe_{0.5}Te_{0.5}$	FM	Isotropic	836	0.01
	NSP		874	
	AFM1	Isotropic	874	0.006
	AFM1	*a*	0.0	2.09
	AFM1	*b*	0.0	2.09
	AFM1	*c*	0.0	2.09
	AFM1	[110]	0.0	2.09
	AFM2	Isotropic	191	2.36
	AFM2	*a*	191	2.36
	AFM2	*b*	191	2.36
	AFM2	*c*	191	2.36
	AFM2	[110]	191	2.36

magnitude of the pseudogap in AFM2 is also similar to that of the nonmagnetic state.[5] On the other hand, in the AFM1 configuration the size of the pseudogap is smaller. As pointed out previously,[5] the pseudogap occurs at an electron count of six per Fe, and the Fermi level lies near the bottom of this pseudogap. Compared to FeSe, FeTe has a higher DOS at the Fermi energy in both AFM1 and AFM2 configurations, as shown in Figs. 2(c) and 2(d). In the ground state, the total DOS at the Fermi energy ($N(E_F)$) is about 8.6 and 1.0 for FeTe and FeSe, respectively. The higher $N(E_F)$ leads FeTe to a stronger magnetic instability like that of $FeTe_{1.125}$.[25]

From the orbital-resolved Fe *d* and chalcogenides *p* PDOS for FeSe and FeTe, it is apparent that the DOS at the Fermi energy is mainly contributed by Fe 3*d* orbitals. For FeSe, Se 4*p* orbitals have a modest hybridization with Fe 3*d* from −5.8 to −3.3 eV, and in FeTe, Te 5*p* orbitals hybridize with Fe 3*d* from −5.2 to −1.7 eV. This is consistent with the trend that Te 5*p* atomic orbitals have higher orbital energies and extend more than those of Se 4*p* atomic orbitals. A remarkable feature is that at the Fermi energy, Se 4*p* orbitals exhibit a gap, whereas Te 5*p* orbitals have a finite contribution to the DOS, which can effectively mediate an Fe-Fe superexchange interaction. Ma *et al.*[11] also noticed that the band formed by Te 5*p* orbitals at the Fermi energy is partially filled, resulting in a large third-nearest neighbor coupling J_3 in FeTe.

B. Evolution of magnetic order in $FeTe_{1-x}Se_x$

We now turn to a discussion of the magnetic behavior in $FeTe_{1-x}Se_x$. There exist two competing (0.5,0.5) and (0.5,0) magnetic orders in this system. In order to obtain a clear understanding of the evolution of the magnetic order with *x*, systems with a Se content *x* at 0.125, 0.25, 0.375, 0.5, 0.625, 0.75, and 0.875 with the substitutional sites randomly chosen were studied. For $FeTe_{1-x0}Se_{x0}$ and $FeTe_{x0}Se_{1-x0}$ at an explicit content *x*0, the Se and Te positions are exchanged. Here, the lattice constants for $FeTe_{1-x}Se_x$ are calculated according to the Vegard law using the experimental lattice constants of pure FeSe and FeTe. The internal parameters were then optimized. The energy differences between the AFM1 and AFM2 configurations, as well as between the corresponding ground state and the NSP case in $FeTe_{1-x}Se_x$, are displayed in Fig. 3 as a function of *x*. One can readily see that the AFM2 phase has a lower energy than the AFM1 phase for $x < 0.18$, suggesting that the (0.5,0) order is stable in this regime. With $x > 0.18$, (positive value of the triangular symbols in Fig. 3), the (0.5,0.5) ordered state (AFM1) becomes more stable. The decrease in the relative energy between the NSP state and the corresponding (AFM1/AFM2) ground state with increasing *x* (Fig. 3) indicates that the magnetic stability in $FeTe_{1-x}Se_x$ becomes weaker as the Se content is increased. This is in consistent with the trend that a SDW instability is considerably stronger in FeTe than in FeSe.[5]

Liu *et al.*[18] divided $Fe_{1.02}Te_{1-x}Se_x$ into three composition regions with distinct physical properties: region I ($0 \leq x < 0.09$) exhibits a long-range AFM order at (0.5,0), and region II ($0.09 < x < 0.29$) exhibits neither long-range AFM order nor bulk superconductivity. In region III ($x > 0.29$), bulk superconductivity is observed. In the $Fe_{1.02}Te_{0.62}Se_{0.38}$ sample, they found that a short-ranged AFM order at (0.5,0) coexists with (0.5,0.5) spin fluctuations, and a spin-gap and resonance form in the spin excitation spectrum.[18] A similar study of $Fe_{1+y}Te_{1-x}Se_x$ showed that magnetic fluctuations at (0.5,0) and (0.5,0.5) coexist over a wide composition range.[15] Our finding of the (0.5,0) order at small *x* is in good agreement with Liu *et al.*'s result in region I.[18] As shown in Fig. 3, (0.5,0.5) and (0.5,0) ordered states have close energies in the region around $x = 0.18$. This result, together with quantum fluctuations and disorder effect in the Se doped system, provides a natural explanation of the absence of long-range magnetic order and

Downloaded 24 Aug 2011 to 166.111.32.163. Redistribution subject to AIP license or copyright; see http://jap.aip.org/about/rights_and_permissions

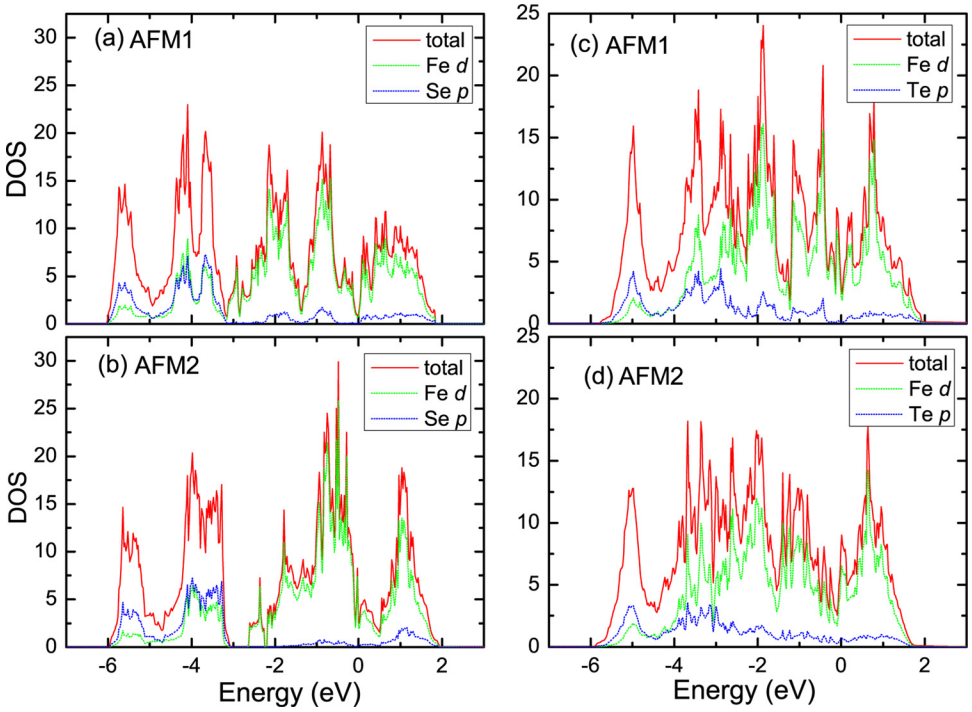

FIG. 2. (Color online) Total electronic DOS and projected Fe 3*d*, Se *p*, and Fe *p* states for FeSe (a), (b) and FeTe (c), (d) in AFM1 and AFM2 spin arrangements. The Fermi level is set at zero.

the coexistence of (0.5,0) and (0.5,0.5) magnetic fluctuations in a wide composition range.[15]

For a better understanding of the origin of the magnetic behavior in $FeTe_{1-x}Se_x$, the Fermi surfaces of the $FeTe_{1-x}Se_x$ system at the Se contents $x = 0.00$, 0.25, 0.5, and 1.00 in the NSP phase are shown in Fig. 4. Similar to findings in other Fe superconductors, the hole-like Fermi surface sheets are centered on the Γ point $[k = (0, 0)]$ and the electron-like Fermi surface sheets at the M point $[k = (0.5,0.5)]$. Note that the present results for FeSe and FeTe agree well with previous studies.[5,22] It is readily seen that the circle around the M point can be mapped onto that at Γ. Thus, the electron-like Fermi surface nested with the hole-like Fermi surface (for arbitrary k_z). The nesting leads to the aforementioned SDW instability observed in FeTe and FeSe at low temperatures.[5,26]

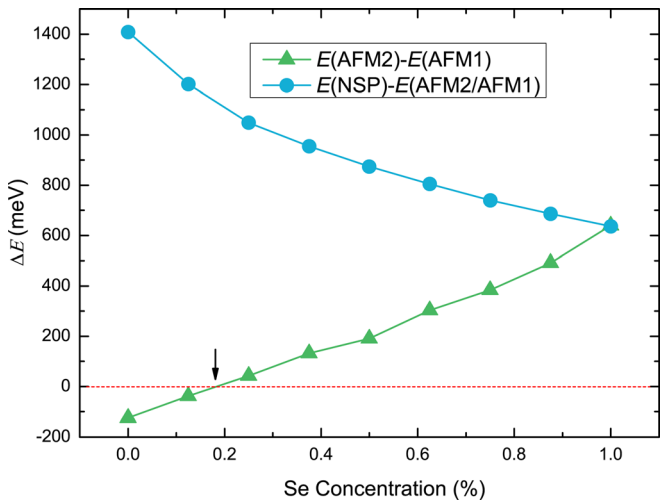

FIG. 3. (Color online) Relative total energies ΔE between AFM1 and AFM2 magnetic configurations as a function of the Se content x for $FeTe_{1-x}Se_x$ alloys. The relative total energies between the NSP state and the corresponding ground state (AFM1/AFM2) are also listed. The black single-head arrow and red dashed line indicate the critical $x = 0.18$ point and $\Delta E = 0$, respectively.

A significant difference between the Fermi surfaces of FeTe and $FeTe_{0.75}Se_{0.25}$ is that the electron-like Fermi surface in the former is a three-dimensional cylinder, whereas that of the latter is more like a two-dimensional circle. Comparing the Fermi surfaces of $FeSe_{0.5}Te_{0.5}$ and FeSe, one sees that the size of the Fermi surface is larger in the former due to a higher DOS at the Fermi level introduced by the Te substitution of Se. As a result, the nesting effect and (0.5,0.5) spin fluctuations necessary for superconductivity are enhanced. The highest superconductivity with $T_c = 15$ K occurs in $FeSe_{0.5}Te_{0.5}$ (Refs. 14 and 27); α-FeSe is a superconductor, but with a lower $T_c = 8$ K.[2] However, this mechanism of superconductivity enhanced by a strong nesting effect failed for FeTe, which has a stronger nesting effect than FeSe (Ref. 5) but does not superconduct.[27] Thus, SDW and superconductivity seem to be competing factors in the Fe(Se,Te) system, and their relationship needs to be studied further.

C. Magnetic and electronic properties of $FeSe_{0.5}Te_{0.5}$

In the following, the discussion is focused on superconducting $FeSe_{0.5}Te_{0.5}$. A crystal model similar to the one used in Ref. 28, in which Se and Te are ordered in layers, was employed. The AMF1, AFM2, FM, and NSP states are examined. The calculations show that after relaxation, the starting FM and AFM1 (not along the easy axis) magnetic configurations collapsed into almost NSP states with remanent moments of 0.01 and 0.006 μ_B per Fe, respectively. The

Downloaded 24 Aug 2011 to 166.111.32.163. Redistribution subject to AIP license or copyright; see http://jap.aip.org/about/rights_and_permissions

magnetic anisotropy energies and magnetic moments are listed in Table I for the AFM1 and AFM2 phases with the axes of magnetization along the *a*, *b*, *c*, and [110] directions. Similar to FeSe and FeTe, $FeSe_{0.5}Te_{0.5}$ does not show any preference regarding the choice of the easy axes. One can notice that after confining the Fe moments along a chosen easy axis, the correct ground state of a single-stripe like AFM1 configuration is obtained. This state is 191 meV lower than the AMF2 counterpart. The moment in AFM1 is 2.09 μ_B, and it is smaller than 2.36 μ_B in AFM2.

The total DOS and projected Fe 3*d*, Te *p*, and Se *p* DOS states for $FeSe_{0.5}Te_{0.5}$ in the AFM1 and AFM2 configurations are shown in Figs. 5(a) and 5(b), respectively. It is clearly shown that both AFM1 and AFM2 have high $N(E_F)$, and more Fe 3*d* itinerant electrons are near the Fermi energy in the former. In order to understand the effect of the magnetization axis, the total DOS for $FeSe_{0.5}Te_{0.5}$ in AFM1 is shown in Fig. 6 with and without consideration of the easy axis. A clear difference is that in the former case, the DOS at the Fermi level is significantly reduced, similar to the case of FeSe discussed above. Similar behavior was also observed for the $La(O_{1-x}F_x)FeAs$ system, in which the DOS at E_F is also reduced strongly in the stripe-like ground state as compared with the nonmagnetic solution.[9] The reduction of the DOS at the Fermi energy weakens the long range interaction (like the Ruderman–Kittel–Kasuya–Yosida interaction) between Fe local spin moments and itinerant electrons, which is consistent with the fact that no long range order except for short range spin fluctuations was observed in $FeSe_{0.416}Te_{0.584}$ (Ref. 3) and $Fe_{1.02}Te_{1-x}Se_x$ samples ($x > 0.29$).[18]

As for the internal structure parameters, the calculated results for FeSe and FeTe in their ground states are, respectively, $x = 0.2573$ and 0.2761, and the corresponding heights above the Fe plane are 1.4198 and 1.7311 Å. For $FeSe_{0.5}Te_{0.5}$ in the ground state, the internal parameters are $x = 0.7133$ and 0.2402 for Se and Te, and the heights are 1.4841 and 1.6899 Å, respectively. These values are consistent with the experimental values of 0.7534 and 0.2916 at 8 K.[28] Compared to the parent alloys FeSe and FeTe, the heights of Se and Te are raised and lowered in $FeSe_{0.5}Te_{0.5}$, respectively. Previous studies[12] showed that the stability of magnetic orders is strongly dependent on the height of the chalcogen atom from the Fe plane. Because FeTe is in the double-stripe (0.5,0) magnetic order at the optimized Te height, the change in the Te height in $FeSe_{0.5}Te_{0.5}$ also plays a role in suppressing the magnetic ordering, in addition to the effect induced by doped Se.

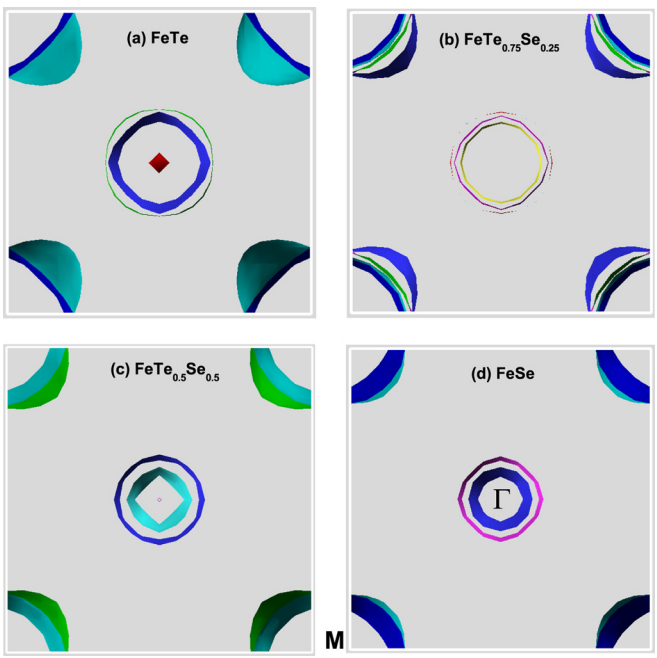

FIG. 4. (Color online) Fermi surfaces of $FeTe_{1-x}Se_x$ as a function of the Se content *x*: (a) FeTe, (b) $FeTe_{0.75}Se_{0.25}$, (c) $FeSe_{0.5}Te_{0.5}$, and (d) FeSe. The hole-like Fermi surface sheets are centered on the Γ point [$k = (0, 0)$], and the electron-like Fermi surface sheets are at the M point [$k = (0.5,0.5)$]. The center and corners of the four square unit cells correspond to the Γ and M points, respectively, as labeled in (d).

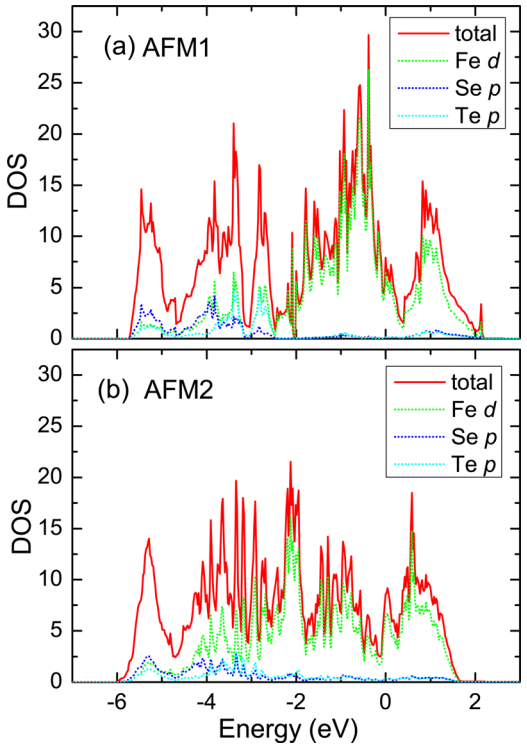

FIG. 5. (Color online) Electronic DOS and projected Fe 3*d*, Te *p*, and Se *p* states for $FeSe_{0.5}Te_{0.5}$ in AFM1 (a) and AFM2 (b) spin arrangements. The Fermi level is set at zero.

Another important structural parameter is the Se(Te)–Fe–Se(Te) bond angle α. For $FeSe_{0.5}Te_{0.5}$ in the ground state, our calculated α (Se–Fe–Se) is 106.5°, approaching the ideal tetrahedral angle of 109.5°, whereas a smaller angle of about 100.5° is obtained in bulk $FeSe_{0.5}Te_{0.5}$ with $T_c \approx 12$ K.[29]

D. Geometry optimization

Geometry optimizations were performed on FeSe, FeTe, and $FeSe_{0.5}Te_{0.5}$ in their ground states with the corresponding magnetic configurations. For FeSe in the AFM1 configuration, a *Cmma* orthorhombic magnetic cell was obtained. The optimized cell parameters and Se atomic position are $a = 5.257$, $b = 5.308$, and $c = 6.261$ Å, and Se is located at (0.0,0.25,0.231). A structural transition is observed from a high-temperature tetragonal structure to an orthorhombic

Downloaded 24 Aug 2011 to 166.111.32.163. Redistribution subject to AIP license or copyright; see http://jap.aip.org/about/rights_and_permissions

structure below 70 K.[30] The orthorhombic super-structure model (space group *Cmma*, $b > a \sim \sqrt{2}a_T$, $c \approx c_T$, where a_T and c_T are the lattice parameters of high-temperature tetragonal unit cell) has been used for FeSe similar to $REFeAsO_{1-x}F_x$.[8,30] The present results compare well with experiments, with the exception of the derivation of the c parameter.

The geometry optimization of FeTe in the AFM2 magnetic order relaxed to a monoclinic cell with a neglectably small magnetic moment of 0.001 μ_B/Fe. In contrast to FeSe and FeTe, the unit cell of $FeSe_{0.5}Te_{0.5}$ remains tetragonal after relaxation, with a residual local magnetic moment of 0.005 μ_B/Fe. These findings are consistent with experimental observations at low temperature where $Fe_{1.076}Te$ has a monoclinic $P2_1/m$ structure below $T_s \approx 75$ K,[10] whereas $FeSe_{0.4}Te_{0.6}$ (Ref. 13) and $FeSe_{0.5}Te_{0.5}$ (Ref. 14) are proved to remain in the tetragonal phase at low temperatures.

E. Spiral spin states for $FeSe_{0.5}Te_{0.5}$ and FeTe

In order to explore the low energy noncollinear magnetic excitations and noncommensurate vector states in superconducting $FeSe_{0.5}Te_{0.5}$, calculations with different spiral spin structures were performed. A unit cell containing four atoms was used. Two spin propagation vectors, $\vec{Q} = (q, q)$ and $(0.5, q)$ (in units of reciprocal lattice vectors), were considered. FM or AFM spin coupling was applied to the two Fe ions in the unit cell at $\vec{Q} = (q, q)$. The momentum dependence of the total energy $E(q)$ for three spin spiral states is shown in Fig. 7. At the commensurate point $\vec{Q} = (0.5,0.5)$, minimum energies were obtained for all three cases, and they were about 0.12 eV (per Fe atom) higher than that of the corresponding ground state. For the AFM case, two anomalies with sudden drops in the total energy were observed at $\vec{Q} = (0.4,0.4)$ and (0.6,0.6). The results of calculations with denser (q, q) points, plotted in the inset, show the two anomalies located at $\vec{Q} = (0.3,0.3)$ and (0.7,0.7), i.e., bracketed symmetrically on either side of $\vec{Q} = (0.5,0.5)$. Similar calculations were also performed for FeTe (shown in the bottom inset of Fig. 7). An energy minimum with two dips on either side was found at the commensurate point $\vec{Q} = (0.5,0.5)$.

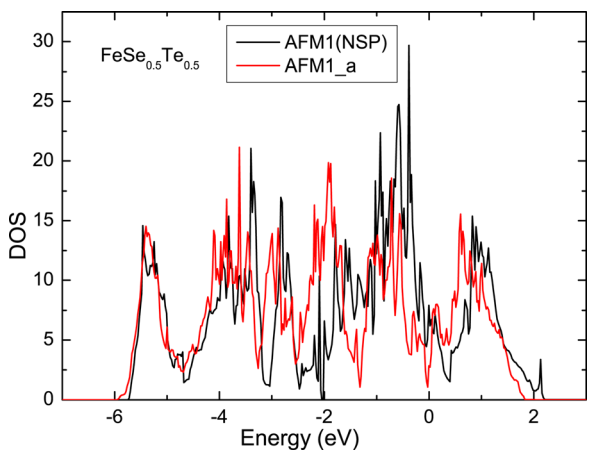

FIG. 6. (Color online) Total DOS of $FeSe_{0.5}Te_{0.5}$ in AFM1 not along the easy axis [AFM1(NSP)] and with the easy axis of magnetisation a (AFM1_a). The former collapses into almost NSP state after no constraint of relaxation. The Fermi level is set at zero.

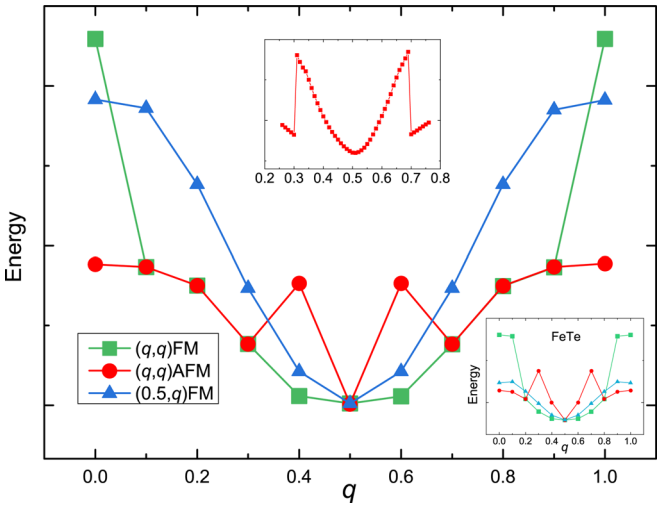

FIG. 7. (Color online) Total energy of $E(q)$ calculated for spin spiral states of $FeSe_{0.5}Te_{0.5}$. Both FM and AFM couplings are considered for the two Fe atoms in the tetragonal unit cell used for our calculations. Two different spiral spin propagation vectors, $\vec{Q} = (q, q)$ and $(0.5, q)$, in units of reciprocal lattice vectors, are adopted.

Experimentally, the spin excitation spectra of $Fe_{1+y}Te_{1-x}Se_x$ (Ref. 18) and $FeTe_{1-x}Se_x$ (Refs. 13 and 14) samples have been studied in detail. A strong quasi-two-dimensional spin resonance was observed at the wave vector $\vec{Q} = (0.5,0.5)$ in superconducting $FeSe_{0.4}Te_{0.6}$.[13] In the ideal superconducting composition of $FeSe_{0.5}Te_{0.5}$,[14] two kinds of excitations were observed: a resonance at the commensurate point $\vec{Q} = (0.5,0.5)$ and two incommensurate fluctuations on either side of this position. It was further found that with different doping concentrations, the resonance point is fixed whereas the incommensurate vector is changed.

Although Fe(Se,Te) and $FeTe_{1+y}$ (with very small y) have different AFM order vectors, the resonance occurs at the same Fermi nesting vector $\vec{Q} = (0.5,0.5)$.[13,14,18] Our spiral magnetic structure calculations show that the minimal energy is obtained at $\vec{Q} = (0.5,0.5)$ for both $FeSe_{0.5}Te_{0.5}$ and FeTe, which is compatible with the Fermi nesting vector but independent of the magnetic ordering vector. Our spiral magnetic states at two kinds of critical points (commensurate and incommensurate) could provide a possible explanation of the momentum dependent spin excitation spectrum.

IV. SUMMARY

Using first principles calculations, the magnetic properties of the Fe(Se,Te) system were investigated systematically. For FeSe and FeTe, our results show that the ground states lie in the single striped (0.5,0.5) and double striped (0.5,0) phases, respectively. It is found that the magnetic anisotropy energy is degenerate in the a, b, c, and [110] directions of an undistorted unit cell for both FeSe and FeTe in the corresponding ground states. The results for the evolution of the magnetic order as a function of the Se content in the $FeTe_{1-x}Se_x$ system show that when $x > 0.18$, the magnetic order switches from double striped (0.5,0) to single striped (0.5,0.5) order. A comparison

Downloaded 24 Aug 2011 to 166.111.32.163. Redistribution subject to AIP license or copyright; see http://jap.aip.org/about/rights_and_permissions

of the Fermi surfaces of $FeSe_{0.5}Te_{0.5}$ and FeSe shows that the substitution of Se by Te enlarges the size of the Fermi surface in $FeSe_{0.5}Te_{0.5}$, and the resulting stronger nesting effect enhances the superconductivity as observed in experiments. Our spiral calculations predict that the lowest energy is obtained at the commensurate point (0.5,0.5), in which the resonance is also observed in the spin excitation spectrum of $FeSe_{0.5}Te_{0.5}$. In addition, two low energy incommensurate excitations were predicted in the vicinity of the $\vec{Q} = (0.5,0.5)$ resonance by the spin spiral calculations.

ACKNOWLEDGMENTS

Z.B.H. was supported by NSFC Grant No. 10974047 and SRFDP Grant No. 20104208110001, and this project is also partly supported by the National Basic Research Program of China (Grant No. 2011CB922200).

[1]Y. Kamihara, T. Watanabe, M. Hirano, and H. Hosono, J. Am. Chem. Soc. **130**, 3296 (2008).
[2]F. C. Hsu, Y. Kamihara, T. Watanabe, M. Hirano, and H. Hosono, Proc. Natl. Acad. Sci. U.S.A. **105**, 14262 (2008).
[3]S. Li, C. Cruz, Q. Huang, Y. Chen, J. Lynn, J. Hu, Y. Huang, F. Hsu, K. Yeh, M. Wu, and P. Dai, Phys. Rev. B **79**, 054503 (2009).
[4]L. Boeri, O. V. Dolgov, and A. A. Golubov, Phys. Rev. Lett. **101**, 026403 (2008).
[5]A. Subedi, L. Zhang, D. J. Singh, and M. H. Du, Phys. Rev. B **78**, 134514 (2008).
[6]M. A. McGuire, A. D. Christianson, A. S. Sefat, B. C. Sales, M. D. Lumsden, R. Jin, E. A. Payzant, D. Mandrus, Y. Luan, V. Keppens, V. Varadarajan, J. W. Brill, R. P. Hermann, M. T. Sougrati, F. Grandjean, and G. J. Long, Phys. Rev. B **78**, 094517 (2008).
[7]Q. Huang, Y. Qiu, W. Bao, M. A. Green, J. W. Lynn, Y. C. Gasparovic, T. Wu, G. Wu, and X. H. Chen, Phys. Rev. Lett. **101**, 257003 (2008).
[8]C. de la Cruz, Q. Huang, J. W. Lynn, J. Li, W. Ratcliff II, J. L. Zarestky, H. A. Mook, G. F. Chen, J. L. Luo, N. L. Wang, and P. Dai, Nature (London) **453**, 899 (2008).
[9]J. Dong, H. J. Zhang, G. Xu, Z. Li, G. Li, W. Z. Hu, D. Wu, G. F. Chen, X. Dai, J. L. Luo, Z. Fang, and N. L. Wang, Europhys. Lett. **83**, 27006 (2008).
[10]W. Bao, Y. Qiu, Q. Huang, M. Green, P. Zajdel, M. Fitzsimmons, M. Zhernenkov, S. Chang, M. Fang, B. Qian, E. Vehstedt, J. Yang, H. Pham, L. Spinu, and Z. Mao, Phys. Rev. Lett. **102**, 247001 (2009).
[11]F. Ma, W. Ji, J. Hu, Z.-Y. Lu, and T. Xiang, Phys. Rev. Lett. **102**, 177003 (2009).
[12]C.-Y. Moon and H. J. Choi, Phys. Rev. Lett. **104**, 057003 (2010).
[13]Y. Qiu, Wei Bao, Y. Zhao, C. Broholm, V. Stanev, Z. Tesanovic, Y. Gasparovic, S. Chang, J. Hu, B. Qian, M. Fang, and Z. Mao, Phys. Rev. Lett. **103**, 067008 (2009).
[14]H. A. Mook, M. Lumsden, A. Christianson, S. Nagler, B. Sales, R. Jin, M. McGuire, A. Sefat, D. Mandrus, T. Egami, and C. Cruz, Phys. Rev. Lett. **104**, 187002 (2010).
[15]M. D. Lumsden, A. Christianson, E. Goremychkin, S. Nagler, H. Mook, M. Stone, D. Abernathy, T. Guidi, G. MacDougall, C. Cruz, A. Sefat, M. McGuire, B. Sales, and D. Mandrus, Nat. Phys. **6**, 182 (2010).
[16]D. N. Argyriou, A. Hiess, A. Akbari, I. Eremin, M. Korshunov, J. Hu, B. Qian, Z. Mao, Y. Qiu, C. Broholm, and W. Bao, Phys. Rev. B **81**, 220503 (2010).
[17]M. D. Lumsden and A. D. Christianson, J. Phys.: Condens. Matter **22**, 203203 (2010).
[18]T. J. Liu, J. Hu, B. Qian, D. Fobes, Z. Mao, W. Bao, M. Reehuis, S Kimber, K. Prokes, S. Matas, D. Argyrion, A. Hiess, A. Rotaru, H. Pham, L. Spinu, Y. Qiu, V. Thampy, A. Savici, J. Rodriguez, and C. Broholm, Nature Mater. **9**, 716 (2010).
[19]J. P. Perdew, K. Burke, and M. Ernzerhof, Phys. Rev. Lett. **77**, 3865 (1996).
[20]G. Kresse and D. Joubert, Phys. Rev. B **59**, 1758 (1999).
[21]G. Kresse and J. Furthmuller, Phys. Rev. B **54**, 11169 (1996).
[22]M. J. Han and S. Y. Savrasov, Phys. Rev. Lett. **103**, 067001 (2009).
[23]Z. Li, J. S. Tse, and C. Q. Jin, Phys. Rev. B **80**, 092503 (2009).
[24]I. I. Mazin, M. D. Johannes, L. Boeri, K. Koepernik, and D. J. Singh, Phys. Rev. B **78**, 085104 (2008).
[25]L. Zhang, D. J. Singh, and M. H. Du, Phys. Rev. B **79**, 012506 (2009).
[26]G. Garbarino, A. Sow, P. Lejay, A. Sulpice, P. Toulemonde, M. Mezouar, and M. Núñez-Regueiro, Europhys. Lett. **86**, 27001 (2009).
[27]K. Yeh, T. Huang, Y. Huang, T. Chen, F. Hsu, P. Wu, Y. Lee, Y. Chu, C. Chen, J. Luo, D. Yan, and M. Wu, Europhys. Lett. **84**, 37002 (2008).
[28]D. Louca, K. Horigane, A. Llobet, R. Arita, S. Ji, N. Katayama, S. Konbu, K. Nakamura, T.-Y. Koo, P. Tong, and K. Yamada, Phys. Rev. B **81**, 134524 (2010).
[29]K. Horigane, H. Hiraka, and K. Ohoyama, J. Phys. Soc. Jpn. **78**, 074718 (2009).
[30]S. Margadonna, Y. Takabayashi, M. McDonald, K. Kasperkiewicz, Y. Mizuguchi, Y. Takano, A. Fitch, E. Suard, and K. Prassides, Chem. Commun., **4**, 5607 (2008), and references therein.

Downloaded 24 Aug 2011 to 166.111.32.163. Redistribution subject to AIP license or copyright; see http://jap.aip.org/about/rights_and_permissions